

SUMOylation protects FASN against proteasomal degradation in breast cancer cells treated with grape leaf extract

Andrea Floris

Cedars-Sinai Medical Center

Michael Mazarei

Cedars-Sinai Medical Center

Xi Yang

Cedars-Sinai Medical Center

Aaron Elias Robinson

Cedars-Sinai Medical Center

Jennifer Zhou

Cedars-Sinai Medical Center

Antonio Barberis

"Consiglio Nazionale delle Ricerche"

Guy D'hallewin

"Consiglio Nazionale delle Ricerche"

Emanuela Azara

"Consiglio Nazionale delle Ricerche"

Ylenia Spissu

"Consiglio Nazionale delle Ricerche"

Ainhoa Iglesias-Ara

Universidad del Pais Vasco Servicios Generales de Investigacion

Sandro Orru

Universita degli Studi di Cagliari Facolta di Medicina e Chirurgia

Maria Lauda Tomasi (✉ marialauda.tomasi@cshs.org)

Cedars-Sinai Medical Center <https://orcid.org/0000-0001-8156-9052>

Research article

Keywords: Antioxidant, breast cancer, FASN, lipid metabolism, polyphenols, protein degradation, protein stability, ubiquitination, SUMOylation

Posted Date: February 26th, 2020

DOI: <https://doi.org/10.21203/rs.2.24639/v1>

License:  This work is licensed under a Creative Commons Attribution 4.0 International License.

[Read Full License](#)

Version of Record: A version of this preprint was published at Biomolecules on March 31st, 2020. See the published version at <https://doi.org/10.3390/biom10040529>.

Abstract

Background: Existing therapeutic strategies for breast cancer are limited by tumor recurrence and drug-resistance. Several epidemiological studies indicate that antioxidant plant-derived compounds such as flavonoids reduce adverse outcomes and have been identified as a potential source of antineoplastic agent with less undesirable side effects. Activation of lipid metabolism is an early event in carcinogenesis and a central hallmark in breast cancer. In fact, inhibition of fatty-acid synthesis in breast cancer results in cytotoxicity that triggers apoptosis. Here, we describe the novel regulation of lipid metabolism in breast cancer cells whereby the protein stability and degradation of fatty-acid synthase (FASN), the key enzyme in de novo fatty-acid synthesis, is regulated by SUMOylation.

Methods: The phenolic characterization were analyzed by Liquid Chromatography-Mass Spectrometry (LCMS). Profile protein contents was evaluated by Mass Spectrometry (LC-MS/MS). The experiments were performed using MCF7, SKBR-3 human carcinoma cell lines and MCF-12A breast epithelial cell line treated with Vermentino hydroalcoholic extract in dose and time course responses. Protein and mRNA levels were analyzed by western blotting/Co-immunoprecipitation (Co-IP) and RT-PCR, respectively. The number of viable cells and the cell-surviving has been detected by MTT and clonogenicity assays. Apoptotic induction was determined by Flow Cytometric assay using Annexin V-FITC and sorted by A FACSC analysis.

Results: We first tested the potential antitumorigenic effects of *Vitis vinifera* L. cv. Vermentino leaf hydroalcoholic extract in MCF-7 and SKBR-3 breast cancer cell lines and found that this compound demonstrated cytotoxic effects. We went on to determine that FASN and UBC9, the sole E2 enzyme required for SUMOylation, were significantly reduced by treatment with the Vermentino extract. Moreover, we found that FASN was SUMOylated in human breast cancer tissues and cell lines. Finally, lack of SUMOylation caused by SUMO2 silencing reduced FASN protein stability.

Conclusion: Altogether, these results suggest that SUMOylation protects FASN against proteasomal degradation and may exert oncogenic activity through alteration of lipid metabolism in breast cancer. Importantly, we found that these effects were significantly inhibited by treatment with Vermentino leaf extract, which supports the additional validation of the therapeutic value of this compound.

Background

Breast cancer is the most common malignant cancer in females worldwide (1). The existing therapeutic strategies for breast cancer, which include surgery, endocrine therapy, and chemotherapy, are limited by tumor recurrence and drug-resistance (2). Therefore, novel approaches are needed to enhance the efficacy of existing therapeutic agents and to improve current clinical protocols.

Adjuvant therapies often attempt to induce cytotoxicity in tumor cells. As tumor cells are known to rely on alternate metabolic processes, such as de novo fatty-acid synthesis, these pathways harbor many potential therapeutic targets. In fact, inhibition of fatty-acid synthesis promotes apoptosis and produces

cytotoxicity, which can trigger cell death (3). A key enzyme in de novo fatty-acid synthesis is fatty-acid synthase (FASN). FASN catalyzes acetyl-CoA and malonyl-Co to form palmitate and a 16-carbon fatty acid (4). FASN is highly expressed in various breast cancer cell lines, including hormone independent lines, such as SKBR-3, and hormone dependent lines, such as MCF-7 (5). FASN can be regulated through genetic modulation and/or nuclear maturation of an isoform of SREBF1 (sterol regulatory element binding transcription factor 1), SREBP1c (sterol regulatory element binding protein 1c). SREBP1c is a transcription factor that binds the FASN promoter and increases the transcription rate of FASN (6). In addition, FASN positively regulates and is regulated by expression of AKT serine/threonine kinase 1 (AKT1). AKT1 activation protects cells from cell death following inhibition of fatty-acid synthesis (7).

Another attractive addition to current clinical protocols is recommendation of a diet high in naturally occurring antioxidants. High consumption of fruits and vegetables containing antioxidative vitamins, carotenoids, and others small molecules with chemo-preventative activity can be an important element of primary cancer prevention (8). Plant pharmacological activity is strongly correlated with natural antioxidants (9). Plant-derived antioxidant compounds, such as flavonoids, reduce adverse outcomes of reactive oxygen and nitrogen species and are a potential source of antineoplastic and cytotoxic agents with fewer undesirable side effects (10–11). Several epidemiological studies indicate that high flavonoid intake is correlated with reduced risk of cancer (12). In vitro studies demonstrate that several mechanisms are linked to flavonoid-mediated cytotoxicity, including cell proliferation inhibition, adhesion, invasion, cell differentiation with simultaneous cell cycle arrest inhibition, and apoptosis (13–14). Flavonoids are a sub-group of more than 5,000 polyphenolic compounds with excellent antioxidant properties that are naturally produced in considerable quantities in fruits and leaves (15). Oxidation to ortho- and para-quinones are the standard aromatic transformation related to the presence of the phenolic hydroxyl, which contributes to antioxidant characteristics (16).

Here, we investigated *Vitis vinifera* L. cv. Vermentino because it is representative of the productive activities of the Sardinian territory and has a unique phenolic profile compared to other vines commonly produced in north Italy. The aim of this study was to explore the potential cytotoxicity of the hydroalcoholic extract of Vermentino leaves as well as the cell signaling pathways implicated in any potential pharmacological effects.

Methods

Cell culture and treatments

The human breast cancer cell lines MCF-7 and SKBR-3 as well as the MCF-12A normal breast epithelial cell line were obtained from the American Type Culture Collection (ATCC, Rockville, MD, USA) and were grown according to instructions provided by the ATCC. These epithelial cell lines were routinely cultured in high glucose DMEM containing 4.5 g/L D-glucose and supplemented with 10% fetal bovine serum and penicillin (100 U/mL)/streptomycin (100 U/mL) at 37°C under 5% CO₂. In this study, cells were exposed to Vermentino leaf hydroalcoholic extract for 16 and 24 h at concentrations of 100, 200, and 400 µg/mL.

In the experiments described below, cells were treated with 60 µg/mL cycloheximide (CHX) or 0.5 µM MG132 (Sigma-Aldrich, St. Louis, Missouri, USA) for 4, 18, and 24 h. The medium was changed after 15 min of MG132 pretreatment.

Human breast tissue specimens

Three normal breast tissues and five breast cancer tissues from surgical reductive mammoplasty and surgical resection of primary breast cancer, respectively, were used (**Supplementary Table 1**). All tissues were immediately frozen in liquid nitrogen for subsequent protein extraction. Written informed consent was obtained from each patient. The study protocol conformed to the ethical guidelines of the 1975 Declaration of Helsinki, as reflected by a prior approval of the study by Cedars-Sinai Medical Center's human research review committee.

Plant material and extraction procedure

Mature leaves of *Vitis vinifera* L. cultivar Vermentino were collected in August from the apical portion of plants cultivated in the collection field of the Institute of Sciences of Food Production (ISPA) in Oristano, Italy. The leaves were immediately put in a portable fridge and cooled to 4°C to be moved to the ISPA laboratories. There, the leaves were rinsed with tap water, ground into a fine powder in liquid nitrogen to avoid the degradation of thermolabile compounds and processed for polyphenol extraction. The powder that was not immediately processed was kept in sterile bags, put under vacuum, and stored in an ultra-freezer at –80°C for further use.

An accelerated solvent extraction was performed following a previously established methodology (38). A solvent of ethanol/water (40/60%) was tested. The extraction was performed in triplicate. After extraction, the ethanol/water extract was subjected to nitrogen flow to remove ethanol and then freeze-dried. The dried extract was weighed and stored at –80°C until analysis. The yield of extraction was calculated as the ratio between “the weight of freeze-dried recover” and “the initial weight of leaf powder used” and expressed as a percentage.

Phenolic characterization of grapevine extract

HPLC-UV analysis

Vermentino extract was filtered through 0.2-µm RC membrane syringe filters (Phenomenex, Torrance, CA, USA). Phenolic compound was analyzed by LC-MS (liquid chromatography-mass spectrometry), according to previously described conditions (39). A DAD (diode array HPLC detector) was used at 280, 320, and 520 nm for quantitative analyses. The quantification of phenolic compound was performed using the external calibration curves according to commercial standards; the quercetin 3-O-(6 acetyl) glucoside content was calculated using a quercetin 3-O glucoside standard curve.

LC-HRMS analysis

High resolution (HR) MS analyses were performed on a QExactive Orbitrap (Thermo Scientific, Bremen, Germany) coupled to 1200 series HPLC (Agilent Technologies, Santa Clara, CA, USA) equipped with a binary pump, a thermostatic autosampler, and a column oven set to 39°C.

To investigate the secondary metabolite profile, the QExactive was equipped with a heated electrospray ionization source (HESI), operating in both positive and negative ion mode. The HESI parameters were: spray voltage, 3.2 kV; sheath gas flow rate, 35 (arbitrary units); auxiliary gas, 10 (arbitrary units); sweep gas, 2 (arbitrary units); and capillary temperature, 300°C. Full MS acquisition was performed with a resolution power of 70,000 full width at half maximum (FWHM) for parent ions and 17,500 for the fragment ions with mass accuracy of 5 ppm. The MS parameters were: AGC target 1e6, maximum injection time (IT) 200 ms, and scan range 100–1,200 m/z. The Xcalibur 3.1.66 software (Thermo Scientific, Bremen, Germany) was used to control the instruments and to process the data. A Gemini C18 (Phenomenex, Torrance, CA, USA) (100 × 2.1 mm, 3 µm, 100Å) was used for chromatographic separation. The flow rate was 0.2 mL/min⁻¹ during a 55-min period with an injection volume of 5 µL. A linear gradient elution of solvent acetic acid 0.2% (A) and acetonitrile (B) was applied with the following program: 0 min, 10% B; 0–20 min, 10–20% B; 20–40 min, 20–40% B; and 40–50 min, 40–70% B. The column was equilibrated for 8 min prior to each analysis. These conditions were adapted from our previous study (39).

Peaks were identified based on their retention time relative to external standards (t_R), UV–vis spectra (200–650 nm), high resolution mass spectra, phytochemical libraries, and reference literature. Quantification of the single phenolic compounds was performed using calibration curves of the respective reference compounds. When reference compounds were not available, the calibration was based on structurally related molecules.

Western blot and co-immunoprecipitation (co-IP)

MCF-7 and SKBR-3 cells were washed with sterile PBS, and then total proteins were extracted with 100 µL of RIPA buffer containing protease inhibitors, as previously described (40). Immunoprecipitation by specific antibodies was performed as previously reported (41). Immunoprecipitated proteins were subjected to western blotting following standard protocols (Amersham BioSciences, Piscataway, NJ, USA), and the membranes were probed for FASN, AKT1, p-AKT1, SUMO1, SUMO2/3, UBC9 (Santa Cruz Biotechnology, Dallas, TX, USA), UBQ (Proteintech, Rosemont, IL, USA), CASP3, CASP9, and β-actin (Sigma-Aldrich). Bands were detected using an enhanced chemiluminescence detection system (Millipore Corporation, Billerica, MA, USA). Quantification of relative band intensity was performed using Quantity One version 4.6.6. basic (Bio-Rad, Hercules, USA), and β-actin was used as a normalizing factor.

Real-time PCR (RT-PCR) analysis

Total RNA was extracted using a Quick-RNA Kit (Zymo Research, Irvine, CA, USA), according to the manufacturer's protocol. The first strand of cDNA was synthesized via reverse transcription by M-MLV Reverse transcriptase (Invitrogen, Carlsbad, CA, USA). Quantitative real-time PCR analysis was performed

using 2 μ L of PCR product. TaqMan probes for human FASN (Fatty-acid synthase) and the Universal PCR Master Mix were purchased from ABI (Foster City, CA, USA). Hypoxanthine phosphoribosyl-transferase 1 (HPRT1) was used as a housekeeping gene. The delta Ct (Δ Ct) obtained was used to find the relative expression of genes, according to the following formula: relative expression = $2^{-\Delta\Delta$ Ct, where $\Delta\Delta$ Ct = Δ Ct of respective genes in experimental groups – Δ Ct of the same genes in control group.

Cell viability

The MTT assay (3-(4,5-dimethylthiazol-2-yl)-2,5-diphenyltetrazolium bromide) (Bimake, Houston, TX, USA) was performed to determine the number of viable cells in culture, as described by the manufacturer. MCF-7 and SKBR-3 cells were plated into 12-well plates at a density of 1×10^5 cells/well in 1 mL of DMEM. Cells were then treated with various concentrations of hydroalcoholic extraction of Vermentino leaves (100, 200, and 400 μ g/mL) for 16 and 24 h. Cell proliferation rates were determined by adding 10 μ L of MTT labeling reagent to each well and incubating at 37°C for 30 min. The absorbance was measured using a plate reader to read the formation of formazan orange dye at 450 nm.

Flow cytometry assay

To determine the effects of Vermentino extract on cell apoptosis, MCF-7 and SKBR-3 cells were seeded at a density of 2×10^5 cells/well in a 6-well plate and incubated at 37°C overnight. The cells were treated with Vermentino extract for 16 or 24 h at concentrations of 100, 200, and 400 μ g/mL. Untreated cells were used as a control. All cells were detached and washed with cooled PBS. After 24 h, the cells were trypsinized (Invitrogen Life Technologies) and analyzed for apoptosis using flow cytometry. The cells were then resuspended in binding buffer containing Annexin V-FITC and propidium iodide (PI) (Beyotime Institute of Biotechnology, Jiangsu, China) and were then incubated for 15 min in a dark room at room temperature. The cells were washed with 200 μ L binding buffer and 10 μ L of PI solution was added immediately prior to the analysis by flow cytometry, as suggested by the manufacturer. A FACS Calibur analyzer (BD Biosciences, San Jose, CA, USA) was used to perform the analysis.

Clonogenicity assay analysis

Clonogenicity assays were performed to determine the cytotoxic effect of the hydroalcoholic extract of Vermentino on breast cancer cell lines. Briefly, MCF-7 and SKBR-3 cells were harvested from a stock culture, and cells were seeded into 12-well plates at a density of 250 cells/well one day before treatment started. The following day, the cells were treated with either the hydroalcoholic extract at concentrations of 100, 200, or 400 μ g/mL and incubated for 16 or 24 h. After approximately 7–10 days of colony formation, colonies were fixed (paraformaldehyde 4% in PBS) and stained with crystal violet solution (Cell Biolab SNC, San Diego, CA, USA). The number of colonies were then counted. The cell-survival fraction was calculated by dividing the number of obtained colonies after treatment by the number of colonies in the control. Data were represented as number of colonies per well.

Proteomic sample preparation

Fifty micrograms of total proteins were extracted from control and 400 µg/mL Vermentino hydroalcoholic extract treated samples in SKBR-3 and MCF-7 cell lines. Proteins were denatured in a solution of 100 mmol/L TRIS-HCL, pH 8 and 8 mol/L urea. Samples were then ultrasonicated for 10 min at intervals of 10 sec on and 10 sec off (QSonica, Newtown, CT, USA) and centrifuged at 16,000 × g for 10 min at 4°C to remove insoluble pellets. The soluble fraction then was reduced with dithiothreitol (15 mM) for 1 h at room temperature and alkylated with iodoacetamide (15 mmol/L) for 30 min at room temperature in the dark. Then, 50 µg protein was diluted to a final concentration of 2 mol/L urea with 100 mmol/L TRIS-HCL, pH 8 and digested overnight on a shaker at 37°C in 3 µg of trypsin/Lys-C mix (Promega, Madison, WI, USA). Samples were de-salted and cleaned using Hydrophobic-Lipophilic Balance (HLB) plates (Oasis, HLB 3 0µm, 5 mg sorbent), (Waters Corporation, Milford, MA, USA).

LC-MS/MS settings

LC-MS/MS was performed on a Dionex Ultimate 3000 NanoLC connected to an Orbitrap Elite (Thermo Fisher) equipped with an EasySpray ion source. The mobile phase A was composed of 0.1% aqueous formic acid, and mobile phase B was composed of 0.1% formic acid in acetonitrile. Peptides were loaded onto the analytical column (PepMap RSLC C18 2 µm, 100 Å, 50 µm i.d. × 15 cm) at a flow rate of 300 nL/min using a linear AB gradient composed of 2–25% A for 185 min, 25–90% B for 5 min, and then an isocratic hold at 90% for 5 min with re-equilibrating at 2% A for 10 min. The temperature was set to 40°C for both columns. Nano-source capillary temperature was set to 275°C, and spray voltage was set to 2 kV. MS1 scans were acquired in the Orbitrap Elite at a resolution of 60,000 full width at half maximum with an automated gain control target of 1 × 10⁶ ions over a maximum of 500 ms. MS2 spectra were acquired for the top 15 ions from each MS1 scan in normal scan mode in the ion trap with a target setting of 1 × 10⁴ ions, an accumulation time of 100ms, and an isolation width of 2 Da. Normalized collision energy was set to 35%, and one microscan was acquired for each spectra.

Preparative data analysis and peptide identification search

The raw MS files were converted to mzXML using MSConvert and searched against the Swiss-Prot reviewed human FASTA database using the COMET, X! Tandem native, and X! Tandem k-score search algorithms (42-43). Precursor and fragment mass tolerance for all of these search algorithms were set to 10 ppm. Cysteine carbamidomethyl was set as a fixed modification, and oxidation of methionine was set as a variable modification for all search algorithms. A maximum of two missed cleavages for all tryptic peptides was allowed, and Target-decoy modeling of peptide spectral matches was performed with peptide prophet (44). Peptides with a probability score of >95% from the entire experimental dataset were imported into Skyline software (45) to establish a library for quantification of precursor extracted ion intensities (XICs). Precursor XICs from each experimental file were extracted against the Skyline library, and peptide XICs with isotope dot product scores >0.8 and with a minimum of two prototypic peptides per protein were filtered for final statistical analysis of proteomic differences (46). Normalization of raw peptide intensities and protein level abundance inference was calculated using the linear mixed effects model built into the open sources MSSTATs (v3.2.2) software suite (47). The mass spectrometry

proteomics data have been deposited to the ProteomeXchange Consortium via the PRIDE [1] partner repository with the dataset identifier PXD016748.

Protein stability assay and half-life determination

Cycloheximide (60 µg/mL) was added to SKBR-3 cells in co-treatment with 400 µg/mL of Vermentino hydroalcoholic extract per well for 4, 18, and 24 h. Protein levels were determined at indicated time points by western blotting, as described above, using the anti-FASN antibody. The relative amount of FASN protein was evaluated by densitometry and normalized to β-actin. Protein half-life was determined for each experiment using linear regression analysis.

Proteasomal activity assays

Proteasomal activity in MCF-7 and SKBR-3 cell lines was determined with luminescent site-specific substrates using the Proteasome-Glo assay (Promega), according to the manufacturer's protocol. Briefly, cells were plated in 96-well plates at 5 × 10³ cells/well and incubated for 24 h. Cells were treated with Vermentino hydroalcoholic extract, at various concentrations (100, 200, and 400 µg/mL) for 16 and 24 h. Cells were assayed using the Proteasome-Glo kit for chymotrypsin-like (Chym-L), trypsin-like (Tr-L), and caspase-like (Casp-L) activity, according to the manufacturer's protocol.

RNA interference

To perform the RNAi experiments, six different predesigned small interfering RNAs (siRNAs) targeting human SUMO1 (#1 sense sequence: 5'-GGAUAGCAGUGAGAUUCActt-3', antisense: 3'-GUGAAUCUCACUGCUAUCctc-5'), (#2 sense sequence 5'-AAGGUGAAUAUAUAAACUCA-3' and antisense: 3'-UGAGUUUAAUAUAUUCACCUU-5'), human SUMO2 (#1 sense sequence: 5'-CCACAUCCUGACUACUACctt-3', antisense: 3'-GGUAGUAGUCAGGAUGUGGtg-5'), (#2 sense sequence: 5'-GCUGUUACAUGUAGGGCAATT-3', antisense: 3'-UUGCCCUACAUGUAACAGCTA -5'), and human SUMO3 (#1 sense sequence: 5'-GGCAGAUCAGAUUCAGGUUtt -3', antisense: 3'-AACCUGAAUCUGAUCUGCCtc -5') were purchased from Ambion (Austin, TX, USA). The siRNA sequence used for silencing of SUMO3 #2 corresponds to the coding region 161–179 (relative to the start codon), as previously described (47) (Dharmacon Research, Inc., Boulder, CO, USA). MCF-7 and SKBR-3 cells were cultured in 6-well plate (0.5 × 10⁶ cells/well) and transfected using RNAiMax (5 µL/well) (Invitrogen, Carlsbad, CA, USA) with SUMO1 siRNA (10 nM), SUMO2 siRNA (10 nM), or SUMO3 siRNA (10 nM) for 48 h for mRNA or protein expression analyses.

Results

Polyphenol phytochemical composition

To determine the phenolic profile of Vermentino, we subjected crude leaf extract to HPLC chromatography. We found that Vermentino leaves contain a mixture of bioactive compounds, which primarily include quercetin 3-O glucoside and isorhamnetin glucoside (**Table 1**).

Vermentino extract lower cell viability in breast cancer cell lines

As phenolic compound, such as flavonoids, have been shown to induce cytotoxicity in cancer cell lines, we evaluated cell viability after treatment with Vermentino hydroalcoholic extract. We treated MCF-7 and SKBR-3 breast cancer cell lines as well as the MCF-12A human breast epithelial cell line and compared the resulting cytotoxicity. All three cell lines were treated with Vermentino hydroalcoholic extract in increasing concentrations of 100, 200, and 400 µg/mL for 16 and 24 h. Vermentino compound showed significant cytotoxic activity at each concentration, with a 50% reduction of viability following treatment of MCF-7 and SKBR-3 cell lines with 400 µg/mL of the hydroalcoholic extract compared to the control (**Figure 1A**). Importantly, MCF-12A cells showed no reduction in viability over time with Vermentino hydroalcoholic extract. Thus, Vermentino hydroalcoholic extract showed slight apoptotic effects on MCF-7 and SKBR-3 breast cancer cells but not on MCF-12A epithelial breast cells.

Vermentino extract lower clonogenicity survival in breast cancer cell lines

To assess the survival and proliferation of MCF-7 and SKBR-3 human breast cancer cells treated with Vermentino hydroalcoholic leaf extract, we performed clonogenicity assays. Colony formation was evaluated with crystal violet stain, and representative colonies are shown in **Figure 1B and 1C**. Vermentino compound was used in concentrations of 100, 200, and 400 µg/mL for 16 and 24 h. The pure hydroalcoholic dilutions of 200 and 400 µg/mL at 24 h were highly toxic and resulted in 48% and 80% reductions in colony formation in MCF-7 cells, respectively, compared to control colonies (**Figure 1B**). Additionally, the ethanolic dilutions of 200 and 400 µg/mL showed 39.1% and 78.3% reductions in colony formation in SKBR-3 cells, respectively, at 24 h compared to control colonies (**Figure 1C**). These results suggest that the Vermentino compound is promising promoter of cytotoxicity in the breast cancer cells tested.

Vermentino extract induce late apoptosis/necrosis in breast cancer cell lines

To examine whether the cytotoxic activity of Vermentino leaf hydroalcoholic extract was due to the induction of apoptosis, cells were exposed to 100, 200, and 400 µg/mL hydroalcoholic extract for 16 and 24 h and stained with Annexin V-FITC and propidium iodide (PI) then analyzed by cytofluorometry. Treatment for 16–24 h with 200 and 400 µg/mL Vermentino leaf hydroalcoholic extract triggered a significant increase in early apoptosis in 20% of MCF-7 and SKBR-3 cells compared to the control (**Figure 2A-B**). Additionally, the percentage of cell necrosis was significantly increased compared to the control after exposure to 100 µg/mL of the leaf hydroalcoholic extract for 16 and 24 h in MCF-7 and SKBR-3 cells (**Figure 3A-B**). Collectively, incubation with Vermentino leaf hydroalcoholic extract for 24 h significantly increased late apoptotic cells by 20% and necrosis by 25% compared to the control in both cell lines, with the greatest effect observed at a dosage of 400 µg/mL. These results indicate that treatment with Vermentino extract increases cell death via late apoptosis and necrosis in both breast cancer cell lines.

To assess the alterations occurring after treatment with Vermentino extract, we performed an unbiased proteomic screen by LC-MS/MS analysis to investigate which cell signaling pathways were involved

causing cytotoxicity. According to the proteomic results, most of the apoptosis pathways were deregulated in breast cancer cell lines after treatment with Vermentino compound (**Supplementary Figure 1; Supplementary Table 2 and 3**).

Vermentino extract induce CASP9 and CASP3 in breast cancer cell lines

To further investigate the apoptotic potential of Vermentino extract on MCF-7 and SKBR-3 breast cancer cell lines, we assessed the expression and cleavage of caspase-9 (CASP9) and caspase-3 (CASP3), which are closely associated with cell death via apoptosis. As shown in **Figure 3A**, pro-caspase-9 protein levels were reduced to 32% and 45% at concentrations of 200 and 400 µg/mL Vermentino hydroalcoholic extract, respectively, after 24 h in MCF-7 cells compared to the control. Consequently, cleaved caspase-9 expression increased by 1.2- at a concentration of 400 µg/mL hydroalcoholic extract compared to the control. Cleavage of caspase-9 implied that apoptosis was induced by Vermentino compounds. Furthermore, pro-caspase-3 activation was induced by exposure to the phytochemical hydroalcoholic extract of Vermentino, resulting in 25% and 45% reductions of pro-caspase-3 compared to the control at concentrations of 200 and 400 µg/mL, respectively, after 24 h. Consistent with activation of the caspase cascade, cleaved caspase-3 was markedly increased by 2.23- and 2.2-fold at a concentration of 400 µg/mL Vermentino hydroalcoholic extract, respectively, after 24 h.

Consistent with our observations in the MCF-7 cell line, Vermentino extract had a strong activation effect on the caspase cascade in SKBR-3 cells. These results indicate that Vermentino hydroalcoholic extract strongly activated pro-caspase-9, which showed a decrease of 35% at a concentration of 200 µg/mL and a decrease of 56% at a concentration of 400 µg/mL after 24 h compared to the control. Cleaved caspase-9 showed increases of 2.4-fold at a concentration of 400 µg/mL Vermentino hydroalcoholic extract compared to the control. Pro-caspase-3 activation was induced by exposure to the hydroalcoholic extract of Vermentino, as evidenced by pro-caspase-3 reductions of 20% and 60% at concentrations of 200 and 400 µg/mL, respectively, after 24 h compared to the control. Cleaved caspase-3 expression increased, implying that cell apoptosis was induced by Vermentino phytochemical compound.

Vermentino extract lower FASN protein level and promote AKT1 signaling in breast cancer cell lines

Our proteomic analysis revealed that FASN is one of the key apoptosis-related proteins that resulted to be downregulated by Vermentino extract (**Supplementary Table 2 and 3**). **Figure 3B** and **Supplementary Figure 2 and 3** show the intensity of the extracted precursors isotopic envelope (M, M + 1, M + 2) of a representative FASN peptide in control and Vermentino hydroalcoholic extract in MCF-7 and SKBR-3 after 24 h of 400 µg/mL treatment. MCF-7 and SKBR-3 cells treated with Vermentino hydroalcoholic extract showed 70% and 20% reductions in FASN peptide intensity, respectively.

To further confirm the effect of Vermentino leaf extract on cell apoptosis, we treated MCF-7 and SKBR-3 cell lines with 100, 200, and 400 µg/mL hydroalcoholic extract for 24 h and examined the protein expression of FASN, AKT1, and p-AKT1. As shown in MCF-7 cells in **Figure 3C**, FASN protein levels decreased by up to 37% at the protein level at a concentration of 400 µg/mL; whereas, AKT1 levels

remained relatively constant compared to the control. In contrast, p-AKT1 showed an increase of 2.6- and 4.17-fold at 200 and 400 µg/mL, respectively, compared to the control. However, FASN mRNA levels showed a slight increase of 1.2- and 1.6-fold at 200 and 400 µg/mL, respectively, compared to the control (**Figure 3C**, left panel). Similar effects were observed in SKBR-3 cells (**Supplementary Figure 2B**). FASN protein levels decreased by 9% and 35% at concentrations of 200 and 400 µg/mL, respectively; whereas, p-AKT1 increased by 3.6- and 4.8-fold at the same respective concentrations compared to the control. Consistent with the data described above, SKBR-3 cells showed little variation in protein levels of AKT1 compared to the control. However, FASN mRNA levels rose significantly in both cell lines (**Supplementary Figure 2B**, left panel). Together, these results indicate that Vermentino hydroalcoholic extract affects FASN at the level of translation rather than transcription.

In addition, proteomic analysis revealed TRAP1 (TNF receptor associated protein 1) significantly downregulated after treatment with Vermentino extract (**Supplementary Table 2 and 3**). TRAP1 is the mitochondrial member of the heat shock protein 90 (HSP90) family that directly interacts with respiratory complexes, regulates mitochondrial permeability transition in response to apoptotic stimuli, and mediates mitochondrial death (31).

Vermentino extract lowers FASN protein expression by activating proteasomal degradation

Based on the observations that FASN was regulated at the post-transcriptional level and was reduced by treatment with Vermentino extract, we next examined the protein synthesis and degradation of FASN protein. First, we treated MCF-7 and SKBR-3 cells with 400 µg/mL Vermentino hydroalcoholic extract for increasing amounts of time. We found that FASN levels were progressively reduced over time. As shown in MCF-7 cells in **Figure 4A**, FASN protein levels fell by 16% and 26% after 18 and 24 h of exposure, respectively, compared to the control. Similarly, FASN protein levels decreased by 29% and 60% in SKBR-3 cells after 18 and 24 h of compound exposure, respectively, compared to the control (**Figure 4A**, right panel). We went on to calculate FASN protein half-life in MCF-7 cells, which decreased from 42.8 ± 7 h in cycloheximide (CHX) treated samples to 23.7 ± 3 h in CHX and Vermentino hydroalcoholic extract co-treated samples, suggesting that FASN synthesis was not affected by Vermentino extract (**Figure 4B**, left panel). Interestingly, loss of FASN protein was significantly reduced by pretreatment with the proteasome inhibitor MG132 (**Figures 4B**, right panel), indicating that protein degradation may be impacted.

We next investigated whether FASN protein degradation was dependent on ubiquitination status. **Figure 4C** shows that treatment with 400 µg/mL Vermentino hydroalcoholic extract for 24 h increased FASN ubiquitination by 3-fold compared to the control. In addition, treatment with MG132 prevented Vermentino-mediated degradation of FASN protein levels in MCF-7 and SKBR-3 cell lines and resulted in intracellular accumulation of ubiquitinated FASN.

Effects of Vermentino extract on proteasomal activity

Because MG132 protected against Vermentino-induced FASN degradation, we next investigated whether proteasomal activity was altered by treatment with the Vermentino compounds by measuring trypsin-like

(Tr-L), caspase-like (Casp-L), and chymotrypsin-like (Chym-L) proteasomal activity. Treatment with hydroalcoholic extract for 16 and 24 h significantly decreased Tr-L activity in MCF-7 (**Supplementary Figure 4A**) and SKBR-3 (**Supplementary Figure 5A**) cell lines in a dose-dependent manner. After 16 and 24 h of treatment, Tr-L activity was reduced most significantly when treated with 400 µg/mL of each compound in both cell lines. Neither of the Vermentino extract had an effect on Casp-L activity in MCF-7 (**Supplementary Figure 4B**) or SKBR-3 (**Supplementary Figure 5B**) cell lines. Although Chym-L activity was decreased in MCF-7 and SKBR-3 cell lines compared to controls by 50%, there was no significant difference across doses or times (**Supplementary Figure 4C** and **5C**, respectively).

Vermentino hydroalcoholic extract lowers UBC9 protein level in human breast cancer cell lines

As no alterations in Casp-L proteasomal activity were observed with either Vermentino leaf extract, we began investigating SUMOylation, a post-translational modification that causes proteasomal degradation in crosstalk with ubiquitination (17). Our proteomic data shows that the sole E2 enzyme driving SUMOylation, ubiquitin-conjugating enzyme E2 I (UBC9), was downregulated by Vermentino treatment in both cell lines (**Supplementary Table 2** and **3**). Interestingly, UBC9 mediates the stability of its target proteins and is upregulated in premalignant conditions (17). Therefore, we evaluated the protein level of UBC9 and found that UBC9 decreased by 80% and 50% in response to 24 h of exposure to 400 µg/mL Vermentino hydroalcoholic extract in MCF-7 and SKBR-3 cell lines, respectively (**Figure 5**). The intensity of the extracted precursor isotopic envelope (M, M+1, M+2) of a representative UBC9 peptide is shown in MCF-7 cells (**Figure 5**, top left panel) and SKBR-3 cells (**Figure 5**, bottom left panel) after treatment with 400 µg/mL Vermentino hydroalcoholic extract for 24 h. MCF-7 and SKBR-3 Vermentino-treated cell lines both showed a 40% reduction in UBC9 M+2 peptide intensity.

SUMOylation mediates FASN protein stability

Modulation of protein SUMOylation or deSUMOylation modification has been associated with regulation of carcinogenesis in breast cancer. Using three different prediction software, we found that FASN was a highly probable target for SUMOylation (**Supplementary Table 4**), thus this led us to examine the in vivo and in vitro SUMOylation of FASN. We found that human breast cancer tissues exhibited high FASN SUMOylation compared to normal breast tissue (**Figure 6A**). Individual silencing of SUMO1, SUMO2, and SUMO3 in MCF-7 cells did not affect FASN mRNA levels, suggesting that SUMOylation affects FASN protein stability at the post-translational level (**Figure 6B**). Western blot analysis further implicated SUMO2 in downregulation of FASN protein level. Specifically, silencing SUMO2 resulted in a 70% drop in FASN protein level compared to control in MCF-7 cells (**Figure 6C**). **Figure 6D** shows that treatment of MCF-7 cells with Vermentino hydroalcoholic extract for 24 h at 400 µg/mL inhibited formation of the SUMOylation complex by lowering UBC9 protein level without affecting SUMO2 protein expression. To provide evidence that FASN requires SUMO2 for stabilization and protection against degradation by the proteasome, MCF-7 cells were treated with CHX for 18 and 24 h in combination with SUMO2 silencing (**Figure 6E**, left panel). Co-treated cells exhibited reductions in FASN protein levels of 70% and 80%, respectively, compared to the control. In contrast, MCF-7 cells treated with MG132 for 18 and 24 h in

combination with SUMO2 silencing did not exhibit a significant drop in FASN protein levels (**Figure 6E**, right panel). Together, these results suggest that SUMO2 is indeed required for FASN stabilization.

Discussion

Many studies have demonstrated positive associations between cytotoxicity in cancer cells and antioxidant activities of plant-derived compounds, such as quercetin, acid gallic, and isorhamnetin (18–19). In this study, we evaluated the potential cytotoxic effects of the hydroalcoholic extract of Vermentino leaves.

HPLC-UV analysis revealed that Vermentino leaf extract have a unique phenol profile, suggesting that they may have cytotoxic capabilities. Indeed, we found that treatment with the extract suppressed cell viability and survival in MCF-7 and SKBR-3 breast cancer cell lines and exerted no significant effect on MCF-12A normal breast epithelial cells. Moreover, cytofluorometric analyses suggested that breast cancer cells were driven toward late apoptosis and necrosis in a dose- and time-dependent manner. The involvement of the apoptotic pathway was further verified by IPA-software, which showed that the most affected canonical biological pathway was apoptosis.

To investigate the potential pathways underlying the cytotoxic activity, we performed proteomic analyses on treated cells and determined that Vermentino leaf extract downregulated fatty-acid synthase (FASN) expression at the protein level. FASN is a key enzyme in fatty-acid biosynthesis and plays an important role in energy homeostasis via β -oxidation (20). Lipids are the main component of the cell membrane and are essential for cell division. Tumor cells endogenously synthesize extra fatty acids via de novo fatty-acid synthesis, which allows them to sustain higher proliferation rates and faster growth (21). Inhibition of FASN induces apoptosis and creates cytotoxicity that is likely to trigger cell death due to the accumulation of Malonyl-CoA (22–23). To evaluate the mechanism underlying induction of apoptosis in MCF-7 and SKBR-3 cells exposed to Vermentino leaf extract, we evaluated caspase-3 and caspase-9 activity. We found that the Vermentino leaf extract induced programmed cell death in the breast cancer cells via modulation of the caspase-dependent pathway. Consistent with our results, elevation of cleaved caspases is a crucial molecular target in chemoprevention (24–25). The involvement of caspase activation in FASN-induced apoptosis was evaluated by western blot. We found that cleaved caspases increased in a dose-dependent manner after 16- and 24-h treatments with Vermentino leaf extract.

FASN expression is regulated by several growth factors, including epidermal growth factor receptor (EGFR), receptor tyrosine-kinase (ERBB2), and steroid hormone receptors (estrogen receptor, progesterone receptor, and androgen receptor) (26). Binding of growth factors and receptors results in activation of the PI3K-AKT transduction pathway. FASN activity and AKT1 activation are modulated in a coregulatory pathway: FASN regulates AKT1 and activated AKT1 regulates FASN. AKT1 activation protects cells against FASN inhibition-induced cell death by increasing transcription of FASN (27–28). Our data shows that Vermentino leaf extract triggered activation of AKT1 via phosphorylation as well as increased FASN mRNA levels in MCF-7 and SKBR-3 cells. Activated AKT1 stimulates FASN expression by gene modulation

of sterol regulatory element-binding protein 1c (SREBP1C), which is a transcription factor that activates FASN by binding to its promoter region (29). Here, we provide evidence that increased AKT1 activation and the related increase in FASN mRNA compensate for Vermentino-induced FASN downregulation.

To further understand the mechanism of FASN reduction, we explored two pathways: protein synthesis and proteasomal degradation. Treatment with cycloheximide (CHX), a known protein synthesis inhibitor, decreased FASN protein expression by locking protein turnover. However, co-treatment with CHX and Vermentino leaf extract enhanced the reduction of FASN compared to CHX alone, suggesting that downregulation of FASN by the compound is independent of protein synthesis. In contrast, pretreatment with the proteasomal degradation inhibitor MG132 protects FASN from degradation during co-treatment with Vermentino leaf extract, suggesting that the extract downregulate FASN accumulation via activation of proteasomal degradation. Indeed, previous work has demonstrated that treatment with chemotherapeutic agents lowers proteasomal activity of the 20 s subunit (30).

Consistent with our data, we found a downregulation of Tr-L and Chym-L activity and no change in Casp-L activity in both cell lines, compared to controls. These results suggest that FASN downregulation is mediated by Casp-L activity, as Casp-L activity was not affected by Vermentino-induced downregulation. FASN inhibitors cause the accumulation of ubiquitinated proteins through an undetermined mechanism (31). Similarly, Vermentino leaf extract increased the ubiquitination of FASN. Although we observed a general reduction in proteasomal activity, affinity for the proteasomal 20 s subunit was increased and FASN degradation was promoted by proteasomal Casp-L activity.

Together, these data suggest a level of crosstalk between the fatty-acid synthesis and proteasomal pathways whereby FASN reduction is mediated by increased ubiquitination. Therefore, Vermentino leaf extract act to modulate FASN expression and degradation via two distinct mechanisms. The first mechanism involves AKT1 activation, which induces transcription of FASN mRNA. The second mechanism promotes FASN degradation via the ubiquitin-proteasome pathway. Our findings suggest that the homeostatic balance in breast cancer cells favors the second pathway and allows Vermentino-induced FASN degradation to outweigh the induction of FASN mRNA transcription.

Cancer cells sustain high proliferation levels by relying on de novo fatty-acid synthesis in addition to glycolysis. Here, we demonstrated that treatment of breast cancer cells with Vermentino leaf extract altered the levels of FASN and disrupted energetic metabolism, resulting in apoptosis. Also, TRAP1 (TNF receptor associated protein 1), molecular chaperone involved in the regulation of energetic metabolism in several cancers, including breast cancer, was significantly downregulated after treatment with Vermentino extract accordingly with the proteomic results (32)(33). This disruption in the Warburg phenotype (34) of cancer cells leads to increased oxygen consumption rates, which cannot be sustained and ultimately lead to cell death. Synergistic effects of Vermentino-induced FASN and TRAP1 downregulation may drive breast cancer cells to apoptotic cell death and exhibited no effect on normal cells.

Our proteomic analysis also revealed strong reduction in UBC9, the sole E2 enzyme that drives SUMOylation. SUMOylation is a small ubiquitin (UB)-related modifier (SUMO) conjugation that is similar

to ubiquitination (17). However, unlike ubiquitination, which normally targets proteins for degradation, SUMOylation regulates protein stability. UBC9 is the only well characterized E2 enzyme in the SUMOylation cycle that transfers activated SUMO to the target protein (35). UBC9 and SUMO are highly expressed in human premalignant conditions in response to low-grade, long-term oxidative stress, suggesting that up-regulation of SUMOylation may be an adaptive response to oxidative stress (36–37). Therefore, antioxidant treatments could be expected to reduce SUMOylation levels. Based on our proteomic results, we hypothesized that FASN may be a target for SUMOylation, contributing to protein stability, in addition it was highly predicted to be SUMOylated. Immunoprecipitation of FASN in breast cancer cells treated with and without Vermentino extract confirmed our hypothesis that UBC9 downregulation results in reduced SUMOylation complex formation. To understand which SUMO protein was interacting with FASN, we silenced SUMO1, SUMO2, and SUMO3 and found that only SUMO2 silencing reduced the FASN protein level without affecting individual SUMO expression. This suggests that UBC9 drives SUMOylation of FASN through SUMO2 and that SUMO2 acts in a protective mechanism to prevent FASN from being targeted for degradation. Silencing SUMO had no effect on transcription of FASN mRNA, demonstrating that FASN downregulation occurs at the post-translational level. To demonstrate that SUMO2 protects FASN against proteasomal degradation, we treated the breast cancer cell lines with a protein synthesis inhibitor (CHX) and a proteasomal degradation inhibitor (MG132) in combination with SUMO2 silencing. We found that, in combination with CHX treatment, SUMO2 silencing reduced FASN protein levels more than SUMO2 silencing alone. Inhibiting proteasomal degradation had no effect on FASN protein expression.

Conclusion

In summary, we have demonstrated for the first time not only that FASN is SUMOylated, but also that Vermentino leaf extract reduce the ability of breast cancer cells to SUMOylate FASN by lowering the UBC9 protein level. These results provide evidence for novel therapeutic capabilities of Vermentino leaf extract in breast cancer.

Abbreviations

FASN
fatty-acid synthase
Acetyl-CoA
acetyl coenzyme A
Malonyl-CoA
malonic acid
SREBF1
sterol regulatory element binding transcription factor 1
SREBP1c
sterol regulatory element binding protein 1c

AKT
protein kinase B
CHX
cycloheximide
HPLC-UV
high performance liquid chromatography ultraviolet
LC-MS
liquid chromatography-mass spectrometry
LC-HRMS
liquid chromatography high resolution mass spectrometry
MS
mass spectrometry
FWHM
full width at half maximum
IT
injection time
PBS
phosphate-buffered saline
RIPA
radioimmunoprecipitation assay buffer
SUMO
small ubiquitin-like modifier
UBC9
Ubiquitin-conjugating enzyme 9
CASP-3
caspase 3
CASP-9
caspase9
PCR
polymerase chain reaction
HPRT1
hypoxanthine phosphoribosyl-transferase
MTT
3-(4,5-dimethylthiazol-2-yl)-2,5-diphenyltetrazolium bromide
V-FITC
annexin V fluorescein isothiocyanate
PI
propidium iodide
FASTA
text-based format for representing protein sequences

Chym-L
chymotrypsin-like
Tr-L
trypsin-like
Casp-L
caspase-like
siRNA
small interfering RNA
M
precursor isotopic
PI3K
phosphoinositide 3-kinase
HSP90
heat shock protein 90
TRAP-1
tumor necrosis factor receptor associated protein 1

Declarations

AVAILABILITY OF DATA AND MATERIALS

Proteomics data have been deposited to the ProteomeXchange Consortium via the PRIDE (1) partner repository with the dataset identifier PXD016748.

ACKNOWLEDGEMENTS

Same as funding sources.

FUNDING

This research was supported by a grant from Cedars-Sinai Medical Center, ACB&P Division.

AUTHOR INFORMATION

Affiliations

Department of Medicine, Cedars-Sinai Medical Center, Los Angeles, California, USA

Andrea Floris, Michael Mazarei, Xi Yang, Jennifer Zhou, Maria Lauda Tomasi

Advanced Clinical Biosystems Research Institute, The Smidt Heart Institute, Cedars-Sinai Medical Center, Los Angeles, California, USA

Aaron Elias Robinson

Institute of Sciences of Food Production (ISPA), National Research Council (CNR), Sassari, Italy Antonio Barberis, Guy D'hallewin, Ylenia Spissu

Institute of Biomolecular Chemistry (ICB), National Research Council (CNR), Sassari, Italy Emanuela Azara

Department of Genetics, Physical Anthropology and Animal Physiology, University of the Basque Country (UPV/EHU), Bilbao, Spain

Ainhoa Iglesias-Ara

Medical Genetics, Department of Medical Sciences and Public Health, University of Cagliari, Cagliari, Italy

Sandro Orrù

Contributions

A Floris performed much of the experiments, analyzed the data and he wrote the manuscript. ML Tomasi obtained the funding for the study and contributed to generating and analyzing the data presented in all Figures. M Mazarei and X Yang generated the data presented in Figure 8,9 and 10. J Zhou generated the data in Figure 4 and 5. S Orru' provided human breast samples and performed the statistical analysis in all Figures. A Barberis, Y Spissu, G D'hallewin and E Azara prepared the grapevine extracts and Phenolic characterization. A Iglesias-Ara contributed to generating and analyzing the data presented in all Figures.

Corresponding author

Correspondence to **Maria Lauda Tomasi**

ETHICS DECLARATIONS

Ethics approval and consent to participate

NA.

Consent for publication

All authors.

Competing interests

The authors declare that they have no competing interests.

References

1) Pilleron S, Sarfati D, Janssen-Heijnen M, Vignat J, Ferlay J, Bray F, Soerjomataram I. Global cancer incidence in older adults, 2012 and 2035: A population-based study. *Int J Cancer*. 2019;144(1):49-58. doi:

10.1002/ijc.31664. Epub 2018 Oct 30.

2) Guarneri V, Conte P. Metastatic breast cancer: therapeutic options according to molecular subtypes and prior adjuvant therapy. *Oncologist*. 2009;14(7):645-56. doi: 10.1634/theoncologist.2009-0078. Epub 2009 Jul 16.

3) Giró-Perafita A, Sarrats A, Pérez-Bueno F, Oliveras G, Buxó M, Brunet J, Viñas G, Miquel TP. Fatty acid synthase expression and its association with clinico-histopathological features in triple-negative breast cancer. *Oncotarget*. 2017;8(43):74391-74405. doi: 10.18632/oncotarget.20152. eCollection 2017 Sep 26.

4) Zhou W, Tu Y, Simpson PJ, Kuhajda FP, "Malonyl-CoA decarboxylase inhibition is selectively cytotoxic to human breast cancer cells. *Oncogene*. 2009;28(33):2979-2987.

5) Chuang HY, Chang YF, Hwang JJ, "Antitumor effect of orlistat, a fatty acid synthase inhibitor, is via activation of caspase-3 on human colorectal carcinoma-bearing animal, *Biomedicine and Pharmacotherapy*. 2011;65(4):286-292,2011.

6) Zhao X, Feng D, Wang Q. Regulation of lipogenesis by cyclin-dependent kinase 8-mediated control of SREBP1. *Journal of Clinical Investigation*. 2012;122:2417-2427.

7) Lee JS, Sul JY, J. Park B. Fatty acid synthase inhibition by amentoflavone suppresses HER2/neu (erbB2) oncogene in SKBR3 human breast cancer cells. *Phytotherapy Research*. 2013;27:713-720.

8) Filaire E, Dupuis C, Galvaing G, Aubretton S, Laurent H, Richard R, Filaire M. Lung cancer: what are the links with oxidative stress, physical activity and nutrition. *Lung Cancer*. 2013;82(3):383-9. doi: 10.1016/j.lungcan.2013.09.009. Epub 2013 Sep 23. Review.

9) Tan BL, Norhaizan ME, Chan LC. ROS-Mediated Mitochondrial Pathway is Required for Manilkara Zapota (L.) P. Royen Leaf Methanol Extract Inducing Apoptosis in the Modulation of Caspase Activation and EGFR/NF- κ B Activities of HeLa Human Cervical Cancer Cells. *Evid Based Complement Alternat Med*. 2018 ;2018:6578648. doi: 10.1155/2018/6578648. eCollection 2018.

10) Sathishkumar P, Gu FL, Zhan Q, Palvannan T, Mohd Yusoff AR. Flavonoids mediated "Green nanomaterials: a novel nanomedicine system to treat various disease-curent trends and future perspective. *Matter. Lett*. 210. 2018;2630. <http://doi.org/10.1016/j.matlet.2017.08.078>.

11) Govindaraju K, Ingels A, Hasan MN, Sun D, Mathieu V, Masi M, Evidente A, Kornienko A. Synthetic analogues of the montanine-type alkaloids with activity against apoptosis-resistant cancer cells. *Bioorg Med Chem Lett*. 2018;28(4):589-593. doi: 10.1016/j.bmcl.2018.01.041. Epub 2018 Feb 2.

12) Sun LR, Zhou W, Zhang HM, Guo QS, Yang W, Li BJ, Sun ZH, Gao SH, Cui RJ Modulation of Multiple Signaling Pathways of the Plant-Derived Natural Products in Cancer. *Front Oncol*. 2019;9:1153. doi: 10.3389/fonc.2019.01153. eCollection 2019. Review.

- 13) Yang L, Xiao B, Hou L, Zhou G, Mo B, Yao D .Bioactive molecule Icariin inhibited proliferation while enhanced apoptosis and autophagy of rat airway smooth muscle cells in vitro. *Cytotechnology*. 2019;71(6):1109-1120. doi: 10.1007/s10616-019-00348-9. Epub 2019 Oct 3.
- 14) Abd El Maksoud AI, Taher RF, Gaara AH, Abdelrazik E, Keshk OS, Elawdan KA, Morsy SE, Salah A, Khalil H. Selective Regulation of B-Raf Dependent K-Ras/Mitogen-Activated Protein by Natural Occurring Multi-kinase Inhibitors in Cancer Cells. *Front Oncol*. 2019;12;9:1220. doi: 10.3389/fonc.2019.01220. eCollection 2019.
- 15) Panche AN, Diwan AD, Chandra SR. Flavonoids: an overview. *J Nutr Sci*. 2016;29;5:e47. doi: 10.1017/jns.2016.41. eCollection 2016.
- 16) Jie Wang, Jianping Xu, Xue Gong, Min Yang, Chunhong Zhang, Minhui Li. Biosynthesis, Chemistry, and Pharmacology of Polyphenols from Chinese Salvia Species: A Review. *Molecules*. 2019;24(1): 155. Published online 2019 Jan 2. doi: 10.3390/molecules24010155 PMID: PMC6337547 PMID: 30609767
- 17) Matassa DS, Agliarulo I, Avolio R, Landriscina M, Esposito F. TRAP1 Regulation of Cancer Metabolism: Dual Role as Oncogene or Tumor Suppressor. *Genes (Basel)*. 2018;5;9(4). pii: E195. doi: 10.3390/genes9040195.
- 18) Hu J, Zhang Y, Jiang X, Zhang H, Gao Z, Li Y, Fu R, Li L, Li J, Cui H, Gao N. ROS-mediated activation and mitochondrial translocation of CaMKII contributes to Drp1-dependent mitochondrial fission and apoptosis in triple-negative breast cancer cells by isorhamnetin and chloroquine. *J Exp Clin Cancer Res*. 2019;38(1):225. doi: 10.1186/s13046019-1201-4.
- 19) Tor YS, Yazan LS, Foo JB, Wibowo A, Ismail N, Cheah YK, Abdullah R, Ismail M, Ismail IS, Yeap SK. Induction of apoptosis in MCF-7 via oxidative stress generation, mitochondria-dependent and caspase-independent pathway by ethyl acetate extract of *Dillenia Sufruticosa* and its chemical profile. *PLoS One* 10 (2015) e0127441
- 20) Jianxiu Yu, Rong deng, Helen H. Zhu, Sharon S. Zhang, Changhong Zhu, Meh Montminy, Roger Davis, Gen-Dheng Feng. Modulation of Fatty Acid Synthase degradation by concerted action of p38 MAP kinase, E3 ligase COP1, and SH2Tyrosine Phosphatase Shp2. *The Journal of Biological Chemistry*. 2013;288(6):3823-3830.
- 21) Bueno MJ, Jimenez-Renard V, Samino S2, Capellades J, Junza A, López-Rodríguez ML, Garcia-Carceles J, LopezFabuel I, Bolaños JP, Chandel NS, Yanes O, Colomer R, Quintela-Fandino M. Essentiality of fatty acid synthase in the 2D to anchorage-independent growth transition in transforming cells. *Nat Commun*. 2019;10(1):5011. doi: 10.1038/s41467-019-13028-1.
- 22) Schley P D, Jijon HB, Robinson L E, Field C J, Mechanisms of omega-3 fatty acid-induced growth inhibition in MDA-MB-231 human breast cancer cells," *Breast Cancer Research and Treatment*. 2005;92(2):187-195.

- 23) Lee J S, Sul JY, Park JB. Fatty acid synthase inhibition by amentoflavone suppresses HER2/neu (erbB2) oncogene in SKBR3 human breast cancer cells," *Phytotherapy Research*. 2013;27:713-720.
- 24) Adedara IA, Olabiyi BF, Idris UF, Onibiyo EM, Farombi EO. Taurine reverse sodium fluoride-mediated increase in inflammation, caspase-3 activity, and oxidative damage along the brain-pituitary-gonad axis in male rats. *Can. J. Physiol. Pharmacol.* 2017;95:1019-1029.
- 25) Chen W, Zhang H, Liu Y. Anti-Inflammatory and Apoptotic Signaling Effect of Fucoxanthin on Benzo(A)PyreneInduced Lung Cancer in Mice. *J Environ Pathol Toxicol Oncol.* 2019;38(3):239-251. doi: 10.1615/JEnvironPatholToxicolOncol.2019030301.
- 26) Baumann J, Wong J, Sun Y, Conklin DS. Palmitate-induced ER stress increases trastuzumab sensitivity in HER2/neupositive breast cancer cells. *BMC Cancer.* 2016;16:551. doi: 10.1186/s12885-016-2611-8.
- 27) Menendez JA, Lupu R. Fatty acid synthase regulates estrogen receptor- α signaling in breast cancer cells. *Oncogenesis* (2017) 6, e299; doi:10.1038/oncsis.2017.4
- 28) Chang L, Fang S, Chen Y, Yang Z, Yuan Y, Zhang J, Ye L, Gu W. Inhibition of FASN suppresses the malignant biological behavior of non-small cell lung cancer cells via deregulating glucose metabolism and AKT/ERK pathway. *Lipids Health Dis.* 2019;18(1):118. doi: 10.1186/s12944-019-1058-8.
- 29) Zhang C, Hu J, Sheng L, Yuan M, Wu Y, Chen L, Wang G, Qiu Z. Ellagic acid ameliorates AKT-driven hepatic steatosis in mice by suppressing de novo lipogenesis via the AKT/SREBP-1/FASN pathway. *Food Funct.* 2019;10(6):34103420. doi: 10.1039/c9fo00284g.
- 30) Gardner RC, Assinder SJ, Christie G. Characterization of peptidyl boronic acid inhibitors of mammalian 20 S and 26 S proteasomes and their inhibition of proteasomes in cultured cells. *Biochem J.* 2000;346:447–454.
- 31) Little JL, Wheeler FB, Constantinos Koumenis, and Steven J. Kridel. Disruption of Crosstalk Between the Fatty Acid Synthesis and Proteasome Pathways Enhances Unfolded Protein Response Signaling and Cell Death. *Mol Cancer Ther.* 2008;7(12):3816-3824. doi:10.1158/1535-7163.MCT-08-0558.
- 32) Kang BH, Plescia J, Dohi T, Rosa J, Doxsey SJ, Altieri DC. Regulation of tumor cell mitochondrial homeostasis by an organelle-specific Hsp90 chaperone network. *Cell.* 2007;131: 257-270.
- 33) Yoshida S, Tsutsumi S, Muhlebach G, Sourbier C, Lee MJ, Lee S, Vartholomaiou E, Tatokoro M, Beebe K, Miyajima N. Molecular chaperone TRAP1 regulates a metabolic switch between mitochondrial respiration and aerobic glycolysis. *Proc. Natl. Acad. Sci.* 2013;110: 1604-1612.
- 34) Lu J, Tan M, Cai Q. The Warburg effect in tumor progression: mitochondrial oxidative metabolism as an anti-metastasis mechanism. *Cancer Lett.* 2015;356(2):156-64. doi: 10.1016/j.canlet.2014.04.001. Epub 2014 Apr 13.

- 35) Johnson ES, Blobel G. Ubc9 is the conjugating enzyme for the ubiquitin-like protein Smt3p. *J Biol Chem.* 1997;272:26799-26702.
- 36) Manza LL, Codreanu SG, Stamer SL, Smith DL, Wells KS, Roberts RL, et al. Global shifts in protein sumoylation in response to electrophile and oxidative stress. *Chem Res Toxicol.* 2004;17:1706-1715.
- 37) Ferhi S, Santaniello S, Zerizer S, Cruciani S, Fadda A, Sanna D, Dore A, Maioli M, D'hallewin G. Total Phenols from Grape Leaves Counteract Cell Proliferation and Modulate Apoptosis-Related Gene Expression in MCF-7 and HepG2 Human Cancer Cell Lines. *Molecules.* 2019; 24(3):612. Published online 2019 Feb 10. doi: 10.3390/molecules24030612.
- 38) Barberis A, Spissu Y, Fadda A, Azara E, Serra PA. Simultaneous amperometric detection of ascorbic acid and antioxidant capacity in orange, blueberry and kiwi juice, by a telemetric system coupled with a fullerene- or nanotubesmodified ascorbate subtractive biosensor. *Biosensors and Bioelectronics.* 2015;6715:214-223.
- 39) Ramani K, Yang HP, Xia M, Iglesias Ara A, Mato JM, Lu SC. Leptin's mitogenic effect in human liver cancer cells requires induction of both methionine adenosyltransferase 2A and 2B. *Hepatology.* 2008;47:521–531
- 40) Pascale RM, Simile MM, De Miglio MR, Muroli MR, Calvisi DF, Asara G, Casabona D, Frau M, Seddaiu MA, Feo F. Cell cycle deregulation in liver lesions of rats with and without genetic predisposition to hepatocarcinogenesis. *Hepatology.* 2002;35(6):1341-50.
- 41) Eng JK, Jahan TA, and Hoopmann MR. Comet: an open-source MS/MS sequence database search tool. *Proteomics.* 2013;13:22-24.
- 42) Robertson C, Ronald CB. TANDEM: matching proteins with mass spectra, *Bioinformatics,* 2004;20:1466-7.
- 43) Keller A, Nesvizhskii AI, Kolker E, and Aebersold R. Empirical statistical model to estimate the accuracy of peptide identifications made by MS/MS and database search. *Anal Chem.* 2002;74: 5383-5392.
- 44) Liebler DC, MacCoss MJ. Skyline: an open source document editor for creating and analyzing targeted proteomics experiments. *Bioinformatics.* 2010;26:966-968.
- 45) Schilling B, Rardin MJ, MacLean BX, Zawadzka AM, Frewen BE, Cusack MP, Sorensen DJ, Bereman MS, Jing E, Wu CC, Verdin E, Kahn CR, MacCoss MJ, and Gibson BW. Platform-independent and label-free quantitation of proteomic data using MS1 extracted ion chromatograms in skyline: application to protein acetylation and phosphorylation. *Mol Cell Proteomics.* 2012;11: 202-214.
- 46) Choi M, Chang CY, Clough T, Broudy D, Killeen T, MacLean B, and Vitek O. MSstats: an R package for statistical analysis of quantitative mass spectrometry-based proteomic experiments. *Bioinformatics.*

47) Lou Y, Yao J, Zereshki A, Dou Z, Ahmed K, Wang H, Hu J, Wang Y, Yao X. NEK2A interacts with MAD1 and possibly functions as a novel integrator of the spindle checkpoint signaling. J Biol Chem. 2004 ;279(19):20049-57. Epub 2004 Feb 20.

Table

Table 1. Quantification of polyphenol in crude extract of grapevine leaves.

Compound	Vermentino (EtOH/H2O)
Myricetin 3-O glucoside	0.11 ± 0.01
Eridictyol 7-glucoside	0.25 ± 0.03
Quercetin 3-O rutinoside	0.20 ± 0.02
Quercetin 3-O galactoside	1.29 ± 0.06
Quercetin 3-O glucoside	5.92 ± 0.10
Kaempferol 3-O galactoside	0.68 ± 0.03
Kaempferol 3-O rutinoside	0.08 ± 0.01
Kaempferol 3-O glucoside	1.64 ± 0.07
Quercetin 3-O-(6 acetyl) glucoside	0.19 ± 0.03
Isorhamnetin glucoside	8.00 ± 0.22
Total	18.36

Supplementary Information

Additional file 1: Supplementary Table 1.pdf

Characteristics of breast cancer tissues from ErbB2-positive patients

Additional file 2: Supplementary Table 2.pdf

List of proteins of vermentino EtOH extract-treated MCF-7 cells

Additional file 3: Supplementary Table 3.pdf

List of proteins of vermentino EtOH extract-treated SKBR-3 cells

Additional file 4: Supplementary Table 4.pdf

Predicted FASN SUMOylation sites

Additional file 5: Supplementary figure legends.docx

Figure legends of supplementary figures

Additional file 6: Supplementary Figure 1.pptx

Vermentino hydroalcoholic extract alters the proteomic profile in MCF-7 and SKBR-3 cell lines

Additional file 7: Supplementary Figure 2.pptx

Vermentino hydroalcoholic extract lowers FASN protein level in SKBR-3 cells

Additional file 8: Supplementary Figure 3.pptx

Vermentino hydroalcoholic extract lowers FASN protein level in MCF-7 and SKBR-3 cell lines

Additional file 9: Supplementary Figure 4.pptx

Vermentino hydroalcoholic extract inhibit trypsin-like and chymotrypsin-like proteasomal degradation in MCF-7 cells

Additional file 10: Supplementary Figure 5.pptx

Vermentino hydroalcoholic extract inhibit trypsin-like and chymotrypsin-like proteasomal degradation in SKBR-3 cells.

Figures

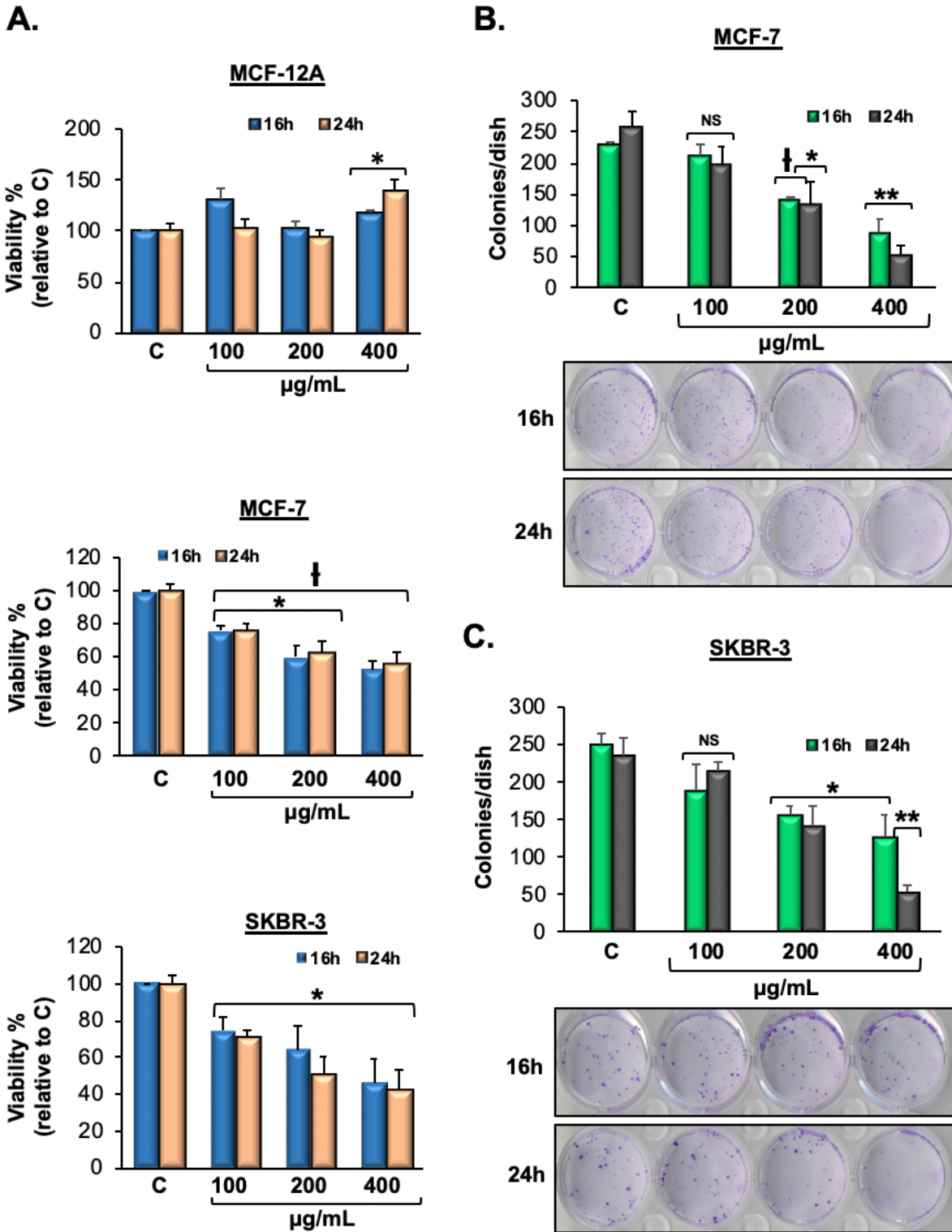
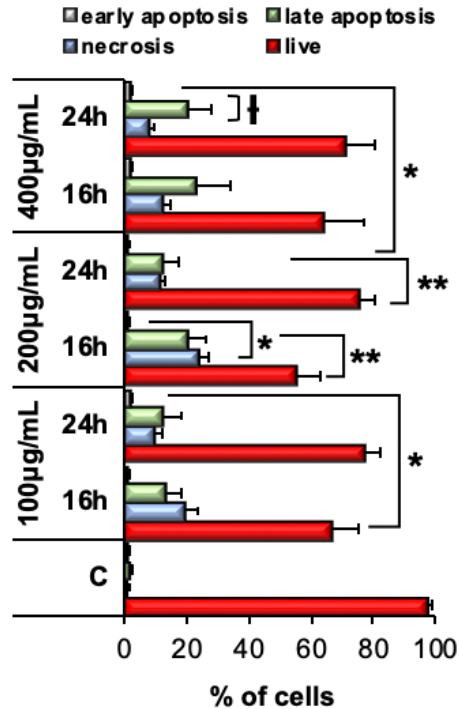
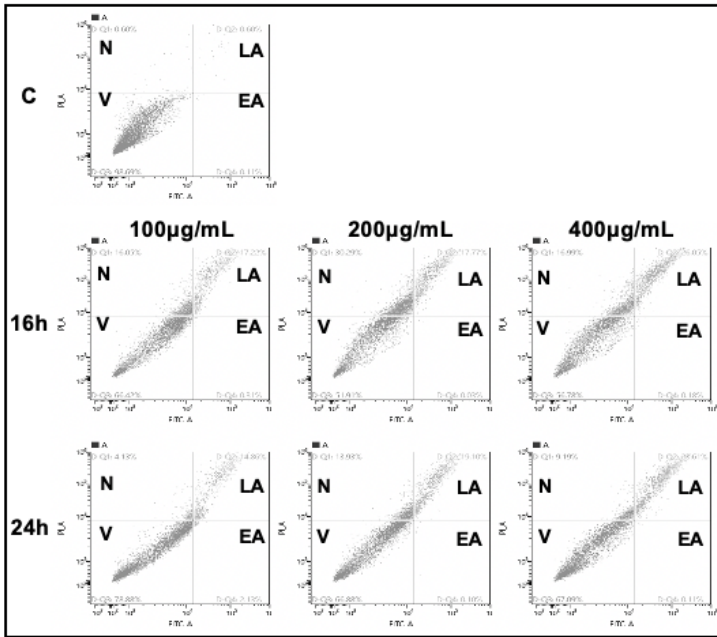


Figure 1

Vermentino extract lower breast cancer cells' viability and clonogenicity in a dose specific response. (A) MTT assay showing MCF-12A SKBR-3 and MCF-7 cells treated with hydroalcoholic extract of Vermentino (100ug/mL, 200ug/mL, or 400ug/mL) for 16 and 24 hrs. The absorbance of the formazan dye was measured at 450nm. The results are expressed as percentage of cell growth (%) ± SE from 3 independent experiments performed in triplicates. *P<0.05 vs. control. **P<0.005 vs. control. (B) Clonogenicity assay

was performed plating cells at density of 0.1×10^6 cells per well in 6-well plates and treated with Vermentino hydroalcoholic extract for 16 and 24hrs at concentrations of 100 μ g/mL, 200 μ g/mL and 400 μ g/mL. Photographs of the petri-dishes in a representative experiment are shown below the histograms. All data are expressed as colonies/dish in 3 independent experiments performed in triplicate. * $P < 0.05$, ** $P < 0.001$, $\square P < 0.0001$ vs the control group.

A. MCF-7



B. SKBR-3

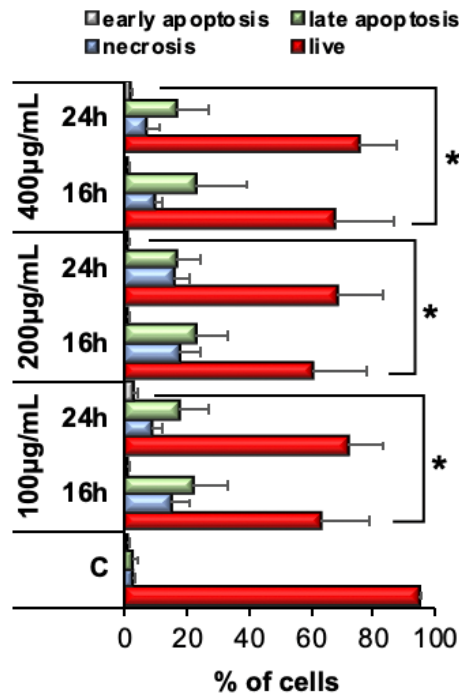
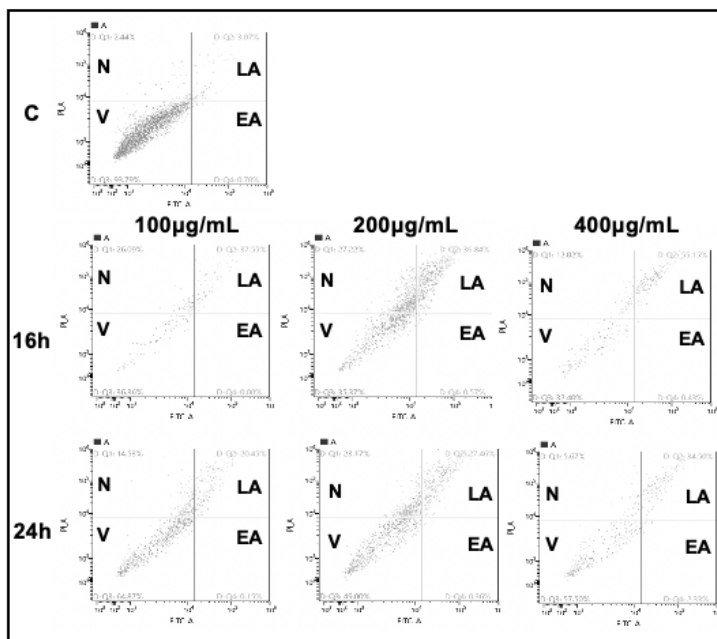


Figure 2

Hydroalcoholic Vermentino extract induces cell death via late apoptosis and necrosis. Apoptotic cell death of MCF-7 and SKBR-3 cells after treatment with Vermentino leaf hydroalcoholic extract after 16 and 24 hours at concentrations of 100ug/mL, 200ug/mL, and 400ug/mL. Apoptotic cells were measured using Annexin V-FITC and propidium iodide staining assay. The lower left quadrant indicates viable cells (V), the upper left quadrant indicates necrosis (N), the upper right quadrant shows late apoptotic cells (LA), and the lower right shows the early apoptotic cells (EA). In the histogram, the values are reported as mean±SE of 3 independent experiments performed in triplicate. *P<0.05, **P<0.001, χ^2 P<0.004 vs. the control group.

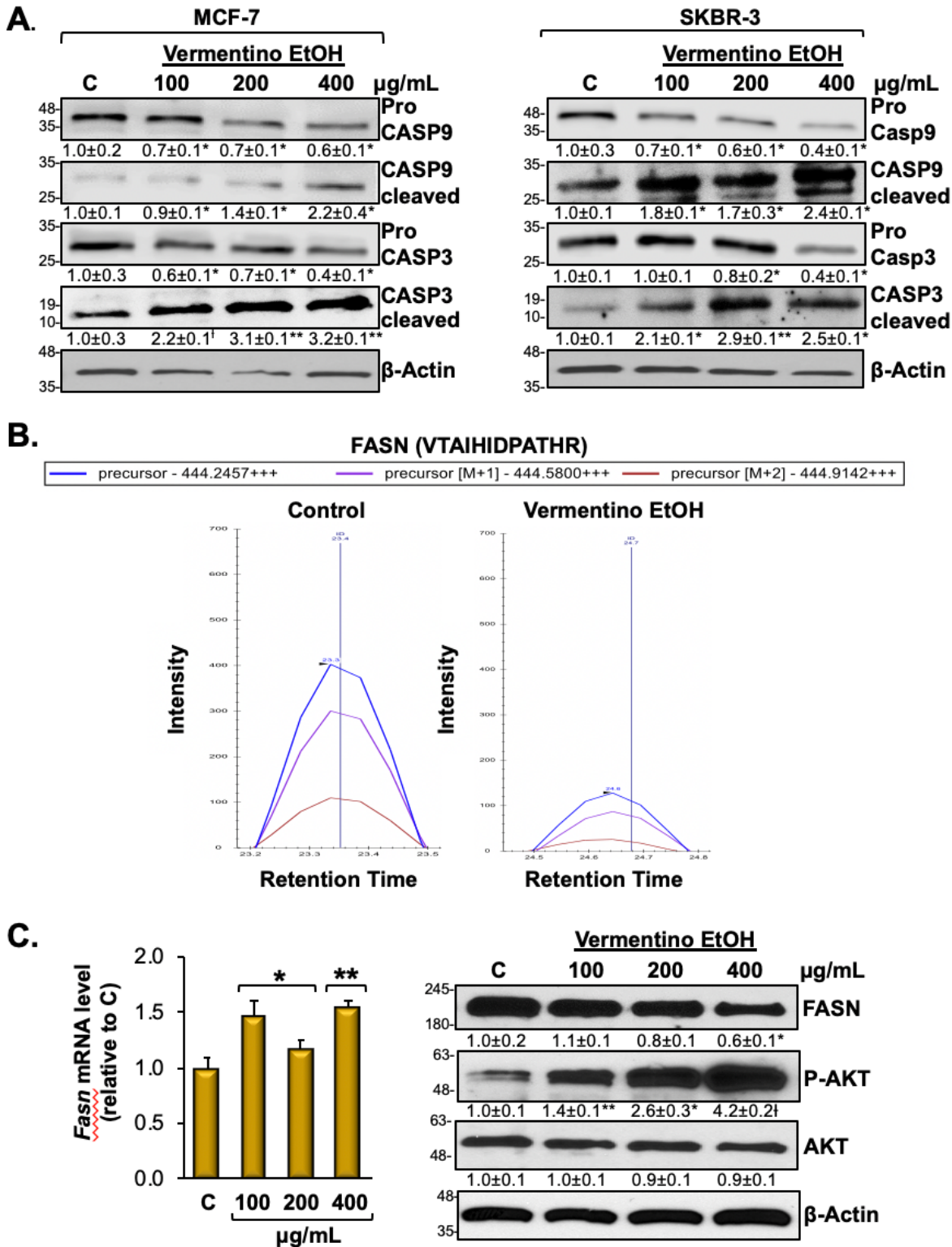


Figure 3

Vermentino extract induces CASP3 and CASP9 activation and lowers FASN protein level. MCF-7 and SKBR-3 cells were plated at density of 0.4×10^6 cells in 6-well/plates and treated with various concentrations of hydroalcoholic extract of vermentino leaves (100ug/mL, 200ug/mL, and 400ug/mL) for 24 hours. (A) Western blot analysis of procaspase-9, cleaved caspase-9, procaspase-3, and cleaved caspase-3 expression in hydroalcoholic extract treated MCF-7 and SKBR-3 cells. Densitometric ratios

normalized to actin are shown below each western blot. Results are expressed as fold of control (mean±SE) from 5 independent experiments. *P<0.05, **P<0.005, ☒P<0.001 vs. control. (B) Intensity of the extracted precursor isotopic envelope (M, M+1, M+2) of a representative FASN peptide VTAIHIDPATHR (MCF-7 cells). All match the theoretical isotopic distribution. (C) mRNA level of FASN was accomplished by using RT-PCR, while protein level was analyzed by Western blot analysis for FASN, AKT and p-AKT (MCF-7 cells). Densitometric ratios normalized to β -actin are shown below the western blot. Results are expressed as a fold of control (mean±SE) from 4 and 3 independent experiments performed in triplicate for mRNA and proteins analysis, respectively. *P<0.05, **P<0.002, ☒P<0.001 vs control.

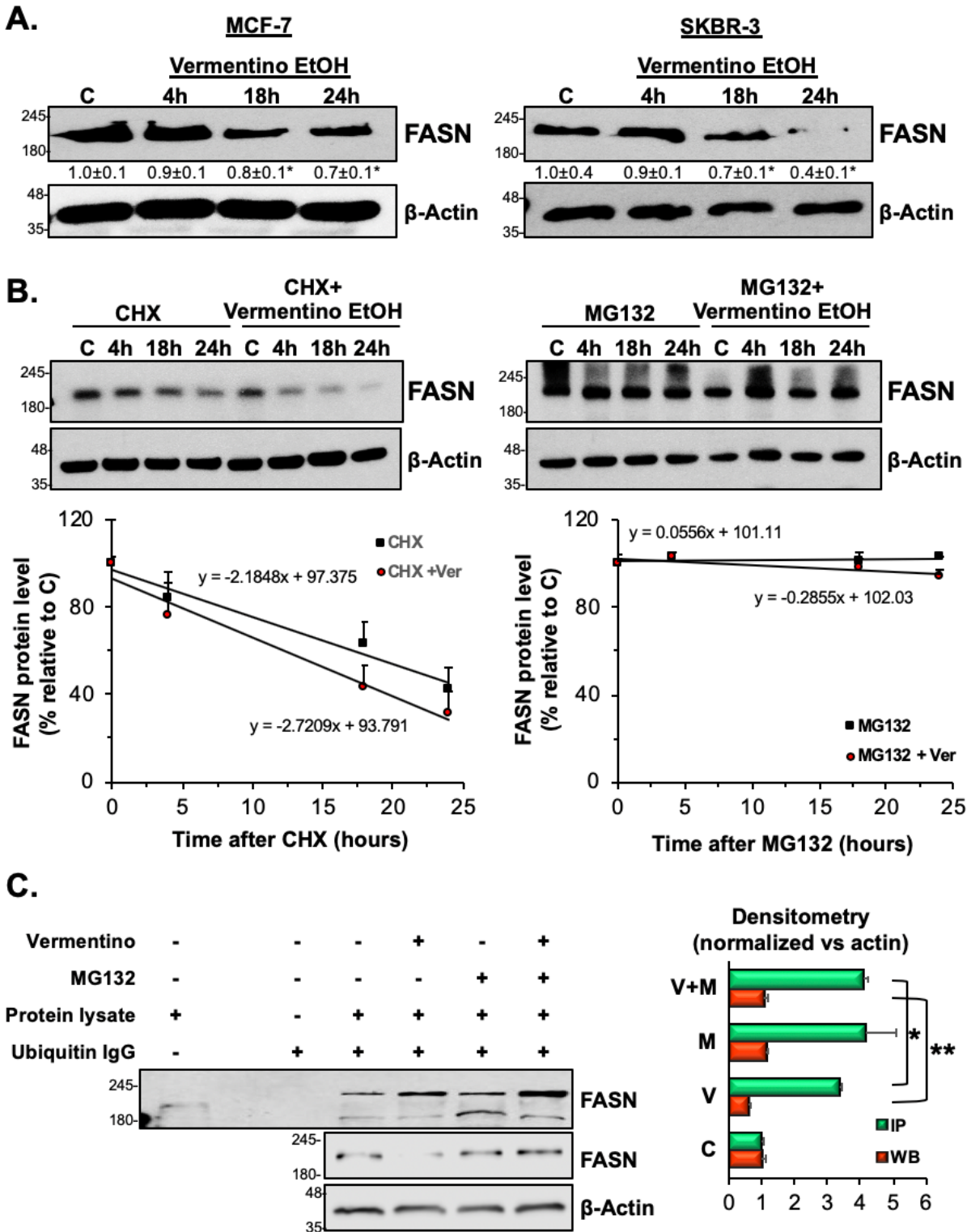


Figure 4

Vermentino hydroalcoholic extract lowers protein stability of FASN. (A) MCF-7 and SKBR-3 cells were treated in time course with 400ug/mL vermentino hydroalcoholic extract. Western blotting results are expressed as fold relative to control from 3 independent experiments and normalized with β -actin.

* $P < 0.05$. (B) FASN protein stability was determined in MCF-7 cells by cycloheximide (CHX) and MG132 treatments when indicated as described in Methods. Linear regression equation was used to calculate

half-life. Results represent mean±SEM from 3 independent experiments expressed as % of respective 0 hour level. *P<0.05, **P<0.008, N.C. $0.71 \leq P \leq 0.91$. (C) Ubiquitination of FASN was analyzed by immunoprecipitation. Densitometric ratios normalized to β -actin are shown next to the western blot. Results are expressed as a fold of control (mean±SE) from 3 independent experiments performed in triplicate. *P<0.005 vs control (WB). **P<0.01 vs control (IP).

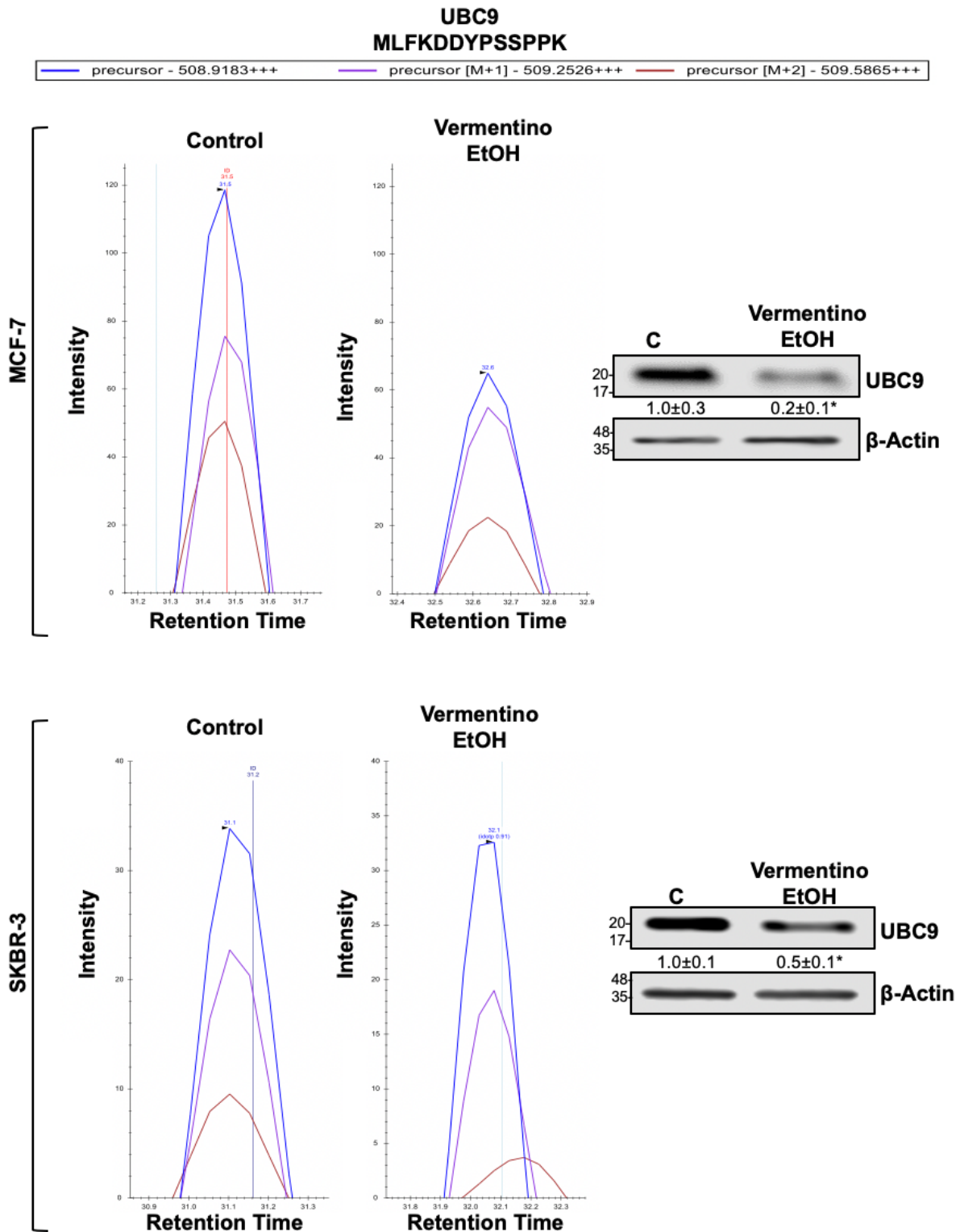


Figure 5

Vermentino hydroalcoholic extract reduces UBC9 protein level in MCF-7 and SKBR-3 cells. Cells were treated with 400ug/mL of extract for 24 hours. Total proteins were extract and analyzed by Mass Spectrometry and Western Blotting UBC9 protein level. (Top and bottom left panels) Intensity of the extracted precursor isotopic envelope (M, M+1, M+2) of a representative UBC9 peptide MLFKDDYPSSPPK in MCF7 and SKBR3 cells treated with Vermentino hydroalcoholic extract. All match the theoretical isotopic distribution. (Top and bottom right panels) Western Blotting of UBC9. Densitometric ratios normalized to actin are shown below each western blot. Results are expressed as fold of control (mean±SE) from 5 independent experiments. *p<0.03 (MCF-7cells), **P<0.05 (SKBR-3 cells) vs. control.

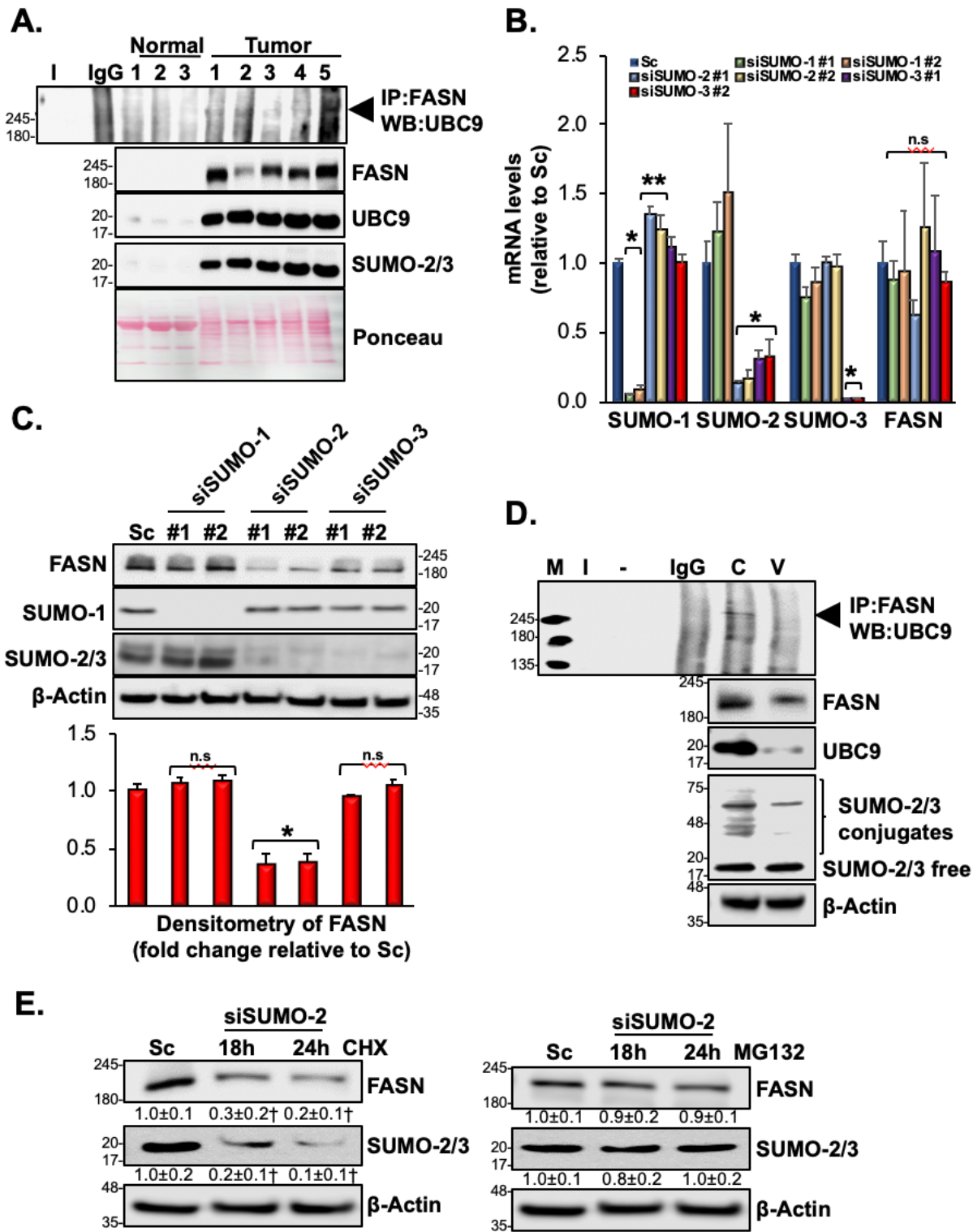


Figure 6

FASN is SUMOylated in vitro and in vivo and Vermentino hydroalcoholic extract inhibits the SUMOylation machinery in MCF-7 cells. (A) FASN immunoprecipitation in 700µg of proteins from human breast normal (n=3) and cancer tissues (n=5) was blotted against UBC9. (B)(C) Cells were transfected with siSUMO-1, siSUMO-2 and siSUMO-3 for 48 hours. SUMOs and FASN expression levels were analyzed by RT-PCR and Western Blotting. (D) MCF-7 cells were treated with 400ug/mL of extract for 24 hours and FASN was

immunoprecipitated to analyze the complex formation with UBC9. (E) Silencing of SUMO-2 was performed (48 hours) in co-treatment with CHX and MG132 for the last 18 and 24 hours. FASN and SUMO-2 protein levels were analyzed by Western Blotting. Densitometric ratios normalized to actin and results are expressed as fold of control (mean±SE) from 3 (B)(E) and 4 (C) independent experiments. *P<0.01, **P<0.04, ***P<0.0003, †P<0.002 vs. Sc.

Supplementary Files

This is a list of supplementary files associated with this preprint. Click to download.

- [SupplementaryTable1.pdf](#)
- [SupplementaryFigure1.pptx](#)
- [SupplementaryFigure2.pptx](#)
- [SupplementaryFigure3.pptx](#)
- [SupplementaryFigure4.pptx](#)
- [SupplementaryFigure5.pptx](#)
- [SupplementaryTable3.docx](#)
- [SupplementaryTable4.docx](#)
- [SupplementaryTable2.docx](#)
- [SUPPLEMENTARYFIGURELEGENDS.docx](#)